

Encoding converters for quantum communication networks

Hua-Xing Xu(许华醒), Shao-Hua Wang(王少华), Ya-Qi Song(宋雅琪), Ping Zhang(张平), and Chang-Lei Wang(王昌雷)

Citation: Chin. Phys. B, 2025, 34 (**5**): 050310. DOI: 10.1088/1674-1056/adcdeb
Journal homepage: http://cpb.iphy.ac.cn; http://iopscience.iop.org/cpb

What follows is a list of articles you may be interested in

Multi-protocol quantum key distribution decoding chip

Chun-Xue Zhang(张春雪), Jian-Guang Li(李建光), Yue Wang(王玥), Wei Chen(陈巍), Jia-Shun Zhang(张家顺), and Jun-Ming An(安俊明)
Chin. Phys. B, 2025, 34 (**5**): 050303. DOI: 10.1088/1674-1056/adb686

Asymmetric mode-pairing quantum key distribution with advantage distillation

Hai-Tao Wang(汪海涛), Chun Zhou(周淳), Yi-Fei Lu(陆宜飞), Chen-Peng Hao(郝辰鹏), Yan-Mei Zhao(赵燕美), Yan-Yang Zhou(周砚扬), Hong-Wei Li(李宏伟), and Wan-Su Bao(鲍皖苏)
Chin. Phys. B, 2025, 34 (**4**): 040305. DOI: 10.1088/1674-1056/adbb5c

Measurement-based entanglement purification for hybrid entangled state

Cheng-Chen Luo(罗程晨), Shi-Pu Gu(顾世浦), Xing-Fu Wang(王兴福), Lan Zhou(周澜), and Yu-Bo Sheng(盛宇波)
Chin. Phys. B, 2025, 34 (**3**): 030307. DOI: 10.1088/1674-1056/adb267

Block-free optical quantum Banyan network based on quantum state fusion and fission

Zhu Chang-Hua (朱畅华), Meng Yan-Hong (孟艳红), Quan Dong-Xiao (权东晓), Zhao Nan (赵楠), Pei Chang-Xing (裴昌幸)
Chin. Phys. B, 2014, 23 (**12**): 120309. DOI: 10.1088/1674-1056/23/12/120309

Distributed wireless quantum communication networks with partially entangled pairs

Yu Xu-Tao (余旭涛), Zhang Zai-Chen (张在琛), Xu Jin (徐进)
Chin. Phys. B, 2014, 23 (**1**): 010303. DOI: 10.1088/1674-1056/23/1/010303

SPECIAL TOPIC — Quantum communication and quantum network

Encoding converters for quantum communication networks

Hua-Xing Xu(许华醒)†, Shao-Hua Wang(王少华), Ya-Qi Song(宋雅琪), Ping Zhang(张平), and Chang-Lei Wang(王昌雷)

China Academy of Electronics and Information Technology, Beijing 100041, *China*

(Received 15 January 2025; revised manuscript received 1 April 2025; accepted manuscript online 17 April 2025)

Quantum communication networks, such as quantum key distribution (QKD) networks, typically employ the measurement-resend mechanism between two users using quantum communication devices based on different quantum encoding types. To achieve direct communication between the devices with different quantum encoding types, in this paper, we propose encoding conversion schemes between the polarization bases (rectilinear, diagonal and circular bases) and the time-bin phase bases (two phase bases and time-bin basis) and design the quantum encoding converters. The theoretical analysis of the encoding conversion schemes is given in detail, and the basis correspondence of encoding conversion and the property of bit flip are revealed. The conversion relationship between polarization bases and time-bin phase bases can be easily selected by controlling a phase shifter. Since no optical switches are used in our scheme, the converter can be operated with high speed. The converters can also be modularized, which may be utilized to realize miniaturization in the future.

Keywords: quantum communication networks, encoding conversion, polarization encoding, time-bin phase encoding

PACS: 03.67.Hk, 03.67.–a

DOI: 10.1088/1674-1056/adcdeb **CSTR:** 32038.14.CPB.adcdeb

1. Introduction

Quantum communication networks can support secure key exchange and information transfer by quantum key distribution (QKD),[1–5] quantum teleportation,[6–8] quantum secure direct communication (QSDC),[9,10] and so on. The typical quantum communication networks are QKD networks, such as integrated space-to-ground quantum communication networks.[11,12] QKD is the most widely studied protocol in quantum cryptography, which Bennett and Brassard proposed in 1984.[13] The first QKD experimental demonstration was realized in 1989.[14] Over the next four decades, quantum communication developed rapidly. The early implementations of QKD systems mainly focused on the communication between two endpoints. With the increase in the number of users who require high-security communication, QKD networks are put forward and widely studied, such as the first QKD network set up by DARPA (Defense Advanced Research Projects Agency),[15,16] the European project SECOQC (Secure Communication based on Quantum Cryptography),[17–19] the Tokyo QKD network,[20] the 2000 km Beijing–Shanghai quantum secret communication trunk, and so on. Up to now, quantum communication networks are composed of lots of QKD systems connected in a point-to-point manner with measurement-resend mechanisms to be compatible with different encoding types and communication protocols. The quantum information can be encoded with various physical properties of photons, such as polarization,[21–26] phase[27–29] and time-bin.[30–33] In a quantum communication network, the quantum communication systems or subnetworks may utilize different quantum encoding methods to be suitable for different communication channels, secure key rates, or cost. To enable direct communication between the users whose encoder and decoder are based on different encoding schemes, a quantum encoding converter is necessary. Therefore, it is necessary to study the conversion scheme between different quantum encoding methods.

There are few researches on quantum encoding conversion schemes in quantum communication. A polarization to phase converter was presented in the patent.[34] The presented converter can convert two sets of conjugate polarization bases (right and left circular polarizations, positive and negative 45° polarizations) into two sets of phase bases ($-\pi/2$ and $\pi/2$, 0 and π). A phase to polarization converter was achieved in Ref. [35]. As the original measurement device independent (MDI) QKD employs the polarization encoding, Alice and Bob can execute the phase encoding MDI QKD by using the phase to polarization converter to adapt the polarization decoder used by Charlie at the photon coincidence measurement end. One of the key components in the converter is the optical switch, which routes the front and back pulses to different paths. However, the speed of the converter is limited by the optical switch.

†Corresponding author. E-mail: xuhuaxing@cetc.com.cn

© 2025 Chinese Physical Society and IOP Publishing Ltd. All rights, including for text and data mining, AI training, and similar technologies, are reserved.

In 2-dimensional quantum systems, information is often encoded in three bases, such as three polarization bases, i.e., rectilinear basis $B_{\rm R}=\{|H\rangle,|V\rangle\}$, diagonal basis $B_{\rm D}=\{|D\rangle,|A\rangle\}$ and circular basis $B_{\rm C}=\{|L\rangle,|R\rangle\}$, and time-bin phase bases, i.e., two phase bases $\{0,\pi\}$, $\{\pi/2,2\pi/3\}$ and time-bin basis $\{|\psi_0\rangle,|\psi_1\rangle\}$. Four states in any two conjugate bases can be selected to implement the BB84 protocol while four or six states in the three bases can be used to realize the RFI protocol.[36] To be compatible with different quantum encoding schemes and quantum communication protocols in quantum communication networks, research on mutual encoding conversion between six polarization states and six time-bin phase states is significant in practice. In this paper, we propose the polarization to time-bin phase and time-bin phase to polarization conversion schemes. Compared with Ref. [34], our scheme can be adopted in QKD systems encoded in any polarization states besides the four polarizations, and one can modulate the conversion relationship simply by controlling a phase shifter. Since no optical switches are used in our scheme, the converter can be operated at high speed. Moreover, the converters can be modularized, which may be utilized to realize miniaturization in the future.

The rest of the paper is organized as follows. In Section 2, we introduce polarization and time-bin phase encodings in quantum communication. In Section 3, we propose the conversion schemes to convert six polarization states to six time-bin phase states and vice versa. We also present the implementations of the converters with optical fiber devices. Finally, the conclusion is given in Section 4.

2. Preliminaries

In this section, we introduce two different kinds of encodings, i.e., polarization encodings and time-bin phase encodings. The introduction of various encodings in this section paves the way for understanding our conversion scheme presented in the following.

2.1. Polarization states

The original QKD scheme in BB84 protocol was achieved by polarization encodings. The qubits are encoded with four states in any two conjugate bases. As represented in Fig. 1(a), there exist three bases conjugate to each other on the Poincaré sphere. They are rectilinear basis $B_{\rm R}=\{|H\rangle,|V\rangle\}$, diagonal basis $B_{\rm D}=\{|D\rangle,|A\rangle\}$ and circular basis $B_{\rm C}=\{|L\rangle,|R\rangle\}$, where $|H\rangle$, $|V\rangle$, $|D\rangle$, $|A\rangle$, $|L\rangle$ and $|R\rangle$ represent horizontal, vertical, 45°, 135°, left-hand and right-hand circular polarizations, respectively.

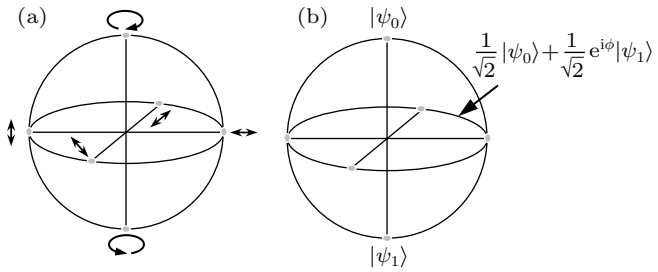


Fig. 1. (a) Six polarization states and (b) six time-bin phase states of three conjugate bases represented on the Poincaré sphere.

Table 1. Six states that can be chosen in the polarization encoding BB84 QKD system.

Basis		X	Y	Z
State	bit "0"	$\|H\rangle$	$\|D\rangle$	$\|L\rangle$
	bit "1"	$\|V\rangle$	$\|A\rangle$	$\|R\rangle$

The relationships of the six states in different bases are

$$|D\rangle=\frac{1}{\sqrt{2}}(|H\rangle+|V\rangle),\ \ |A\rangle=\frac{1}{\sqrt{2}}(|H\rangle-|V\rangle),$$
$$|L\rangle=\frac{1}{\sqrt{2}}(|H\rangle+\mathrm{i}\,|V\rangle),\ \ |R\rangle=\frac{1}{\sqrt{2}}(|H\rangle-\mathrm{i}\,|V\rangle). \quad (1)$$

Note that the encoding states in the BB84 scheme should be in two conjugate bases. Therefore, any two of $B_{\rm R},B_{\rm D},B_{\rm C}$, often called X, Y, Z bases, can be used. By convention, bit "0" can be encoded by the polarization states $|H\rangle$, $|D\rangle$ and $|L\rangle$, while bit "1" can be encoded by the polarization states $|V\rangle,|A\rangle$ and $|R\rangle$, as listed in Table 1.

2.2. Time-bin phase states

The time-bin phase states include two time-bin states and four phase states. In a time-bin phase encoding BB84 QKD system, the two bases are the time-bin basis and a phase basis, or two phase bases. The time-bin basis (Z basis) includes two states $|\psi_0\rangle=|1\rangle_{\rm E}|0\rangle_{\rm L}$ and $|\psi_1\rangle=|0\rangle_{\rm E}|1\rangle_{\rm L}$, where E and L denote the early and late modes, respectively. The general form for a phase encoding qubit is $|\psi\rangle=1/\sqrt{2}(|\psi_0\rangle+e^{i\phi}|\psi_1\rangle)$, with $\phi=\{0,\pi/2,\pi,3\pi/2\}$. In the Z basis, Alice encodes the bit "0" or "1" by states $|\psi_0\rangle$ or $|\psi_1\rangle$. In the X basis, Alice encodes the bit "0" or "1" by states $1/\sqrt{2}(|\psi_0\rangle+|\psi_1\rangle)$ or $1/\sqrt{2}(|\psi_0\rangle-|\psi_1\rangle)$. In the Y basis, Alice encodes the bit "0" or "1" by states $1/\sqrt{2}(|\psi_0\rangle+\mathrm{i}\,|\psi_1\rangle)$ or $1/\sqrt{2}(|\psi_0\rangle-\mathrm{i}\,|\psi_1\rangle)$. The three bases based on time-bin phase encoding are listed in Table 2.

Table 2. Six states that can be chosen in time-bin phase coding BB84 QKD system.

Basis	Z	X	Y
ϕ	–	$\{0,\pi\}$	$\{\pi/2,3\pi/2\}$
State bit "0"	$\|\psi_0\rangle=\|1\rangle_{\rm E}\|0\rangle_{\rm L}$	$1/\sqrt{2}(\|\psi_0\rangle+\|\psi_1\rangle)$	$1/\sqrt{2}(\|\psi_0\rangle+\mathrm{i}\,\|\psi_1\rangle)$
State bit "1"	$\|\psi_1\rangle=\|0\rangle_{\rm E}\|1\rangle_{\rm L}$	$1/\sqrt{2}(\|\psi_0\rangle-\|\psi_1\rangle)$	$1/\sqrt{2}(\|\psi_0\rangle-\mathrm{i}\,\|\psi_1\rangle)$

The idea of encoding qubits using the phase of photons was first proposed by Bennett in Ref. [37]. Figure 2 shows the practical realization of a QKD system based on phase encoding with two asymmetric Mach–Zehnder interferometers at Alice and Bob ends, where the phase ϕ is the relative phase introduced by the two phase modulators, i.e., $\phi = \phi_A - \phi_B$. As shown in Fig. 1(b), the poles denote the time-bin states which can be generated by the interferometer, where the first beam splitter is replaced by a switch. When the coupling ratio of the beam splitter is 50:50, the phase states are on the equator. The azimuth angle of the Poincaré sphere represents the relative phase ϕ.[38] Therefore, the time-bin phase encoding and the polarization encoding are formally isomorphic and there exist conversion schemes in theory.

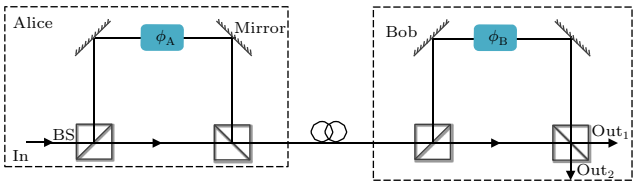


Fig. 2. Phase encoding BB84 scheme with Mach–Zehnder interferometers.

3. Schemes

In quantum communication, quantum information can be encoded using various physical properties of photons, such as polarization and time-bin phase. In certain application scenarios, one encoding method is usually more convenient than others. For example, the information of quantum communication systems is often encoded by time-bin phase in optical fiber whereas by polarization in free space. So, in the scenario of multi-user quantum networks over the wide area, quantum communication may be established between users with different encoding methods, and it is meaningful to develop a universal encoding conversion scheme that can be compatible with different encoding methods.

3.1. Polarization to time-bin phase conversion scheme

Since time-bin phase encoding is formally isomorphic to polarization encoding, conversion schemes between them exist. Here we propose a converter to transform six polarization states into six time-bin phase states, as seen in Fig. 3.

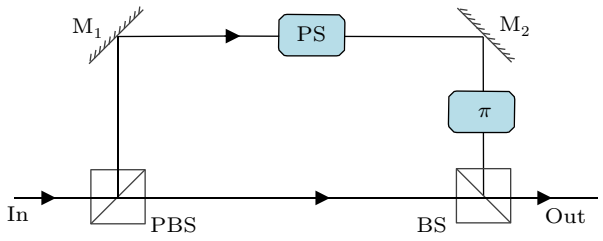


Fig. 3. Schematic of the polarization to time-bin phase converter. The PBS is a polarization beam splitter, the BS is a beam splitter, M$_1$ and M$_2$ are mirrors, the PS is a phase shifter, and the "π" performs the conversion $|V\rangle \to |H\rangle$.

The polarization to time-bin phase converter is composed of a polarization beam splitter (PBS), two arms, a phase shifter (PS), a π-polarization rotator, and a beam splitter (BS). Theoretically, the converter can be regarded as a polarization decoder and a time-bin phase encoder. The PBS acts as the polarization decoder and divides different polarization pulses into the two unbalanced arms. The two arms, the PS and the BS act as the phase encoder, which is similar to an unbalanced-arm interferometer in a time-bin phase encoding QKD system. The function of the π-polarization rotator is to transform $|V\rangle$ to $|H\rangle$. We assume that the input pulse is one of the six polarization states ($|H\rangle$, $|V\rangle$, $|D\rangle$, $|A\rangle$, $|L\rangle$ and $|R\rangle$). After passing through the PBS, the component $|H\rangle$ of the input pulse goes along the lower arm while the component $|V\rangle$ goes along the upper arm. The two unbalanced arms lead to time delay between the two components and the π-polarization rotator makes the polarization along the two arms the same. Then, through the converter, the earlier pulse and the later pulse have the same polarization, and polarization states will be transformed into time-bin phase states. The phase of the component $|V\rangle$ is modulated by the PS to compensate for phase drift caused by the environment or to select the conversion relationship between polarization bases and time-bin phase bases. The converter is described in detail as follows.

When a horizontal polarization state $|H\rangle$ is input, it transfers through the PBS and goes along the short arm. Then, $|H\rangle$ will be the early mode and we have a state $|H\rangle_E|0\rangle_L$ in the output port. The evolution of the input state $|H\rangle$ is

$$|H\rangle \xrightarrow{\text{PBS}} |H\rangle_E|0\rangle_L \xrightarrow{\text{BS}} \frac{1}{\sqrt{2}}|H\rangle_E|0\rangle_L, \tag{2}$$

where $|0\rangle_L$ denotes that there is no photon in the late mode. When a vertical polarization state $|V\rangle$ is input, it transfers through the PBS and goes along the long arm. Specifically, a phase of $\pi/2$ is introduced in the reflected path of the PBS and the BS respectively. Therefore, the state transferred along the long arm acquires an additional phase π. After the π-rotator, the output state will become $-|0\rangle_E|H\rangle_L$. The evolution of the input state $|V\rangle$ is

$$|V\rangle \xrightarrow{\text{PBS}} \mathrm{i}\,|0\rangle_E|V\rangle_L \xrightarrow{\pi} \mathrm{i}\,|0\rangle_E|H\rangle_L \xrightarrow{\text{BS}} -\frac{1}{\sqrt{2}}|0\rangle_E|H\rangle_L. \tag{3}$$

The polarization to time-bin phase conversion scheme transfers the X basis in polarization encoding to the Z basis in time-bin phase encoding.

When inputting a 45° polarization state $|D\rangle$, the PBS splits it into two modes. The evolution of the input state $|D\rangle$ is

$$\begin{aligned} |D\rangle &\xrightarrow{\text{PBS}} \frac{1}{\sqrt{2}}(|H\rangle_E|0\rangle_L + \mathrm{i}\,|0\rangle_E|V\rangle_L) \\ &\xrightarrow{\pi} \frac{1}{\sqrt{2}}(|H\rangle_E|0\rangle_L + \mathrm{i}\,|0\rangle_E|H\rangle_L) \\ &\xrightarrow{\text{BS}} \frac{1}{2}(|H\rangle_E|0\rangle_L - |0\rangle_E|H\rangle_L). \end{aligned} \tag{4}$$

In the similar way, the 135° polarization state $|A\rangle$ can be transformed to $(1/2)(|0\rangle_{\rm E}|H\rangle_{\rm L}+|H\rangle_{\rm E}|0\rangle_{\rm L})$ in the output port. From Table 2, we can find that the polarization to time-bin phase conversion scheme transfers the Y basis in polarization encoding to the X basis in time-bin phase encoding.

When inputting a left-hand circular polarization state $|L\rangle$, the PBS splits it into two modes. The evolution of the input state $|R\rangle$ is

$$\begin{aligned}|L\rangle &\xrightarrow{\rm PBS} \frac{1}{\sqrt{2}}(|H\rangle_{\rm E}|0\rangle_{\rm L}+{\rm i}\cdot{\rm i}\,|0\rangle_{\rm E}|V\rangle_{\rm L})\\ &\xrightarrow{\pi} \frac{1}{\sqrt{2}}(|H\rangle_{\rm E}|0\rangle_{\rm L}-|0\rangle_{\rm E}|H\rangle_{\rm L})\\ &\xrightarrow{\rm BS} \frac{1}{2}(|H\rangle_{\rm E}|0\rangle_{\rm L}-{\rm i}\,|0\rangle_{\rm E}|H\rangle_{\rm L}).\end{aligned} \tag{5}$$

Similarly, the right-hand circular polarization state $|R\rangle$ becomes $1/2(|H\rangle_{\rm E}|0\rangle_{\rm L}+{\rm i}\,|0\rangle_{\rm E}|H\rangle_{\rm L})$ in the output port. Therefore, the polarization to time-bin phase conversion scheme transfers the Z basis in polarization encoding to the Y basis in time-bin phase encoding.

In the analysis above, the PS is set to be zero (or a number to compensate the phase drift). If the PS is set to some other value, the encoding conversion will be different. For example, we take a phase shift induced by $\pi/2$ as an example. The evolution of polarization states in the X basis is

$$|H\rangle \xrightarrow{\rm PBS} |H\rangle_{\rm E}|0\rangle_{\rm L} \xrightarrow{\rm BS} \frac{1}{\sqrt{2}}|H\rangle_{\rm E}|0\rangle_{\rm L}, \tag{6}$$

$$\begin{aligned}|V\rangle &\xrightarrow{\rm PBS} {\rm i}\,|0\rangle_{\rm E}|V\rangle_{\rm L} \xrightarrow{{\rm PS}(\pi/2)} -|0\rangle_{\rm E}|V\rangle_{\rm L}\\ &\xrightarrow{\pi} -|0\rangle_{\rm E}|H\rangle_{\rm L} \xrightarrow{\rm BS} -\frac{\rm i}{\sqrt{2}}|0\rangle_{\rm E}|H\rangle_{\rm L},\end{aligned} \tag{7}$$

when the PS introduces a phase shift of $\pi/2$, the converter transfers the X basis in polarization encoding to the Z basis in time-bin phase encoding. The evolution of polarization states in the Y basis is

$$\begin{aligned}|D\rangle &\xrightarrow{\rm PBS} \frac{1}{\sqrt{2}}(|H\rangle_{\rm E}|0\rangle_{\rm L}+{\rm i}\,|0\rangle_{\rm E}|V\rangle_{\rm L})\\ &\xrightarrow{{\rm PS}(\pi/2)} \frac{1}{\sqrt{2}}(|H\rangle_{\rm E}|0\rangle_{\rm L}-|0\rangle_{\rm E}|V\rangle_{\rm L})\\ &\xrightarrow{\pi} \frac{1}{\sqrt{2}}(|H\rangle_{\rm E}|0\rangle_{\rm L}-|0\rangle_{\rm E}|H\rangle_{\rm L})\\ &\xrightarrow{\rm BS} \frac{1}{2}(|H\rangle_{\rm E}|0\rangle_{\rm L}-{\rm i}\,|0\rangle_{\rm E}|H\rangle_{\rm L},\end{aligned} \tag{8}$$

$$|A\rangle \xrightarrow{\rm converter} \frac{1}{2}(|0\rangle_{\rm E}|H\rangle_{\rm L}+{\rm i}\,|H\rangle_{\rm E}|0\rangle_{\rm L}). \tag{9}$$

The converter transfers the Z basis in polarization encoding to the X basis in time-bin phase encoding, i.e., $|L\rangle\rightarrow|0\rangle$, $|R\rangle\rightarrow|\pi\rangle$. Similarly, we can get the states' evolution for other introduced phases. For π, the conversions are

$$\begin{aligned}&|H\rangle\rightarrow|E\rangle,\ \ |V\rangle\rightarrow|L\rangle,\\ &|D\rangle\rightarrow|0\rangle,\ \ |A\rangle\rightarrow|\pi\rangle,\\ &|L\rangle\rightarrow|\pi/2\rangle,\ \ |R\rangle\rightarrow|3\pi/2\rangle.\end{aligned} \tag{10}$$

For $3\pi/2$, the conversions are

$$\begin{aligned}&|H\rangle\rightarrow|E\rangle,\ |V\rangle\rightarrow{\rm i}\,|L\rangle,\\ &|D\rangle\rightarrow|\pi/2\rangle,\ |A\rangle\rightarrow|3\pi/2\rangle,\\ &|L\rangle\rightarrow|\pi\rangle,\ |R\rangle\rightarrow|0\rangle.\end{aligned} \tag{11}$$

When the PS introduces a phase $3\pi/2$, the Z basis in polarization encoding is transformed into the X basis in time-bin phase encoding. And the bit "0" encoded by $|L\rangle$ is turned to $|\pi\rangle$, which corresponds to the bit "1", so bit flip happens. The conversion results with different phase shifts are listed in Table 3.

Table 3. The conversion results with different additional phases introduced by PS.

Phase of PS	0		$\pi/2$		π		$3\pi/2$	
	Basis	Bit flip?	Basis	Bit flip?	Basis	Bit flip?	Basis	Bit flip?
Polarization	$X\rightarrow Z$	no	$X\rightarrow Z$	no	$X\rightarrow Z$	no	$X\rightarrow Z$	no
↓	$Y\rightarrow X$	yes	$Y\rightarrow Y$	yes	$Y\rightarrow X$	no	$Y\rightarrow Y$	no
Time-bin phase	$Z\rightarrow Y$	yes	$Z\rightarrow X$	no	$Z\rightarrow Y$	no	$Z\rightarrow X$	yes

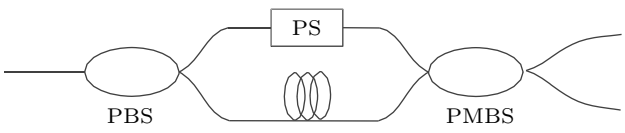


Fig. 4. Schematic of the polarization to time-bin phase converter based on commercial fiber-optic devices.

As seen in Fig. 4, the conversion scheme above can be easily constructed by using commercial fiber-optic components. The converter contains a PBS, a PS, a polarization-maintaining beam splitter (PMBS), and two unbalanced arms. The short arm and the long arm are constituted by the polarization-maintaining fiber (PMF). Both the slow (or fast) axes of the two arms' PMFs are connected to the two output ports of the PBS and the two input ports of the PMBS. Because of the coupling between the slow (or fast) axes of the arms' PMFs and the input ports of the PMBS, there is no need for a π-rotator or other polarizers to unify the polarizations. It can be observed that the structure of the converter in our

scheme is much simpler than that of Ref. [34], and our scheme also contains the conversion of time-bin states.

3.2. Time-bin phase to polarization conversion schemes

We propose a time-bin phase to polarization conversion scheme in this section. The schematic diagram of the converter is shown in Fig. 5, where the time-bin phase to polarization conversion scheme is approximately the inverse of the polarization to time-bin phase conversion scheme.

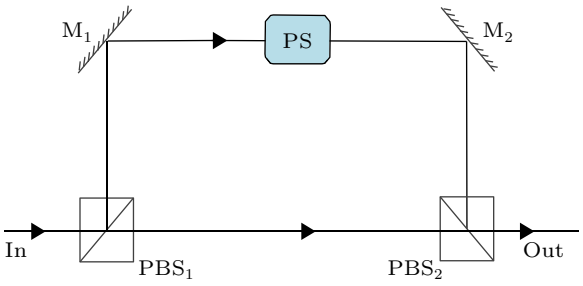


Fig. 5. Schematic of the time-bin phase to polarization conversion scheme.

To see how the converter works, we study the evolution of the input states. Keeping the polarization of the incident light 45° to the polarization direction of the PBS_1, the four phase states $|0\rangle$, $|\pi/2\rangle$, $|\pi\rangle$ and $|3\pi/2\rangle$ are

$$|\mathrm{in}\rangle = \frac{1}{\sqrt{2}}(|T\rangle - \mathrm{e}^{\mathrm{i}\varphi_1}|T+\Delta T\rangle), \tag{12}$$

where $\varphi_1 \in \{0, \pi/2, \pi, 3\pi/2\}$. $|T+\Delta T\rangle$ denotes the state that passes along the long arm of the encoder interferometer and ΔT is the time delay caused by the different lengths of the two arms.

As shown in Fig. 5, when passing through the PBS_1, each input phase state is transformed to the earlier and the later pulses due to the unbalanced arms. Here we set the time delay between the two arms to ΔT, and the evolution of the input state is

$$\begin{aligned}
&\frac{1}{\sqrt{2}}\left(|T\rangle - \mathrm{e}^{\mathrm{i}\varphi_1}|T+\Delta T\rangle\right)\\
\xrightarrow{\mathrm{PBS}_1}\ &\frac{1}{2}\left(|H\rangle|0\rangle - \mathrm{e}^{\mathrm{i}\varphi_1}|H_{T+\Delta T}\rangle|0\rangle\right)\\
&+\frac{\mathrm{i}}{2}\left(|0\rangle|V_{T+\Delta T}\rangle - \mathrm{e}^{\mathrm{i}\varphi_1}|0\rangle|V_{T+2\Delta T}\rangle\right)\\
\xrightarrow{\mathrm{PBS}_2}\ &\frac{1}{2}\left(|H\rangle|0\rangle - \mathrm{e}^{\mathrm{i}\varphi_1}|H_{T+\Delta T}\rangle|0\rangle\right)\\
&-\frac{1}{2}\mathrm{e}^{\mathrm{i}\varphi_2}\left(|0\rangle|V_{T+\Delta T}\rangle - \mathrm{e}^{\mathrm{i}\varphi_1}|0\rangle|V_{T+2\Delta T}\rangle\right),
\end{aligned} \tag{13}$$

where φ_2 is the phase shift modulated by the PS, and $\varphi_2 = 0$ is set for example. Among the three peaks in the output port, only the middle peak is a superposition state. Then we only concentrate on the evolution of the middle peak. It is represented as

$$\begin{aligned}
|\mathrm{out}\rangle &= -\frac{1}{2}\left[\mathrm{e}^{\mathrm{i}\varphi_1}|H\rangle + \mathrm{e}^{\mathrm{i}\varphi_2}|V\rangle\right]\\
&= -\frac{1}{2}\left[\mathrm{e}^{\mathrm{i}\varphi_1}|V\rangle + |H\rangle\right].
\end{aligned} \tag{14}$$

According to Eq. (14), the states in the output port under different input polarization states are

$$\begin{aligned}
|\mathrm{out}\rangle_{\varphi_1=0} &= -\frac{1}{2}(|H\rangle + |V\rangle),\\
|\mathrm{out}\rangle_{\varphi_1=\pi/2} &= -\frac{\mathrm{i}}{2}(|H\rangle - \mathrm{i}|V\rangle),\\
|\mathrm{out}\rangle_{\varphi_1=\pi} &= \frac{1}{2}(|H\rangle - |V\rangle),\\
|\mathrm{out}\rangle_{\varphi_1=3\pi/2} &= \frac{\mathrm{i}}{2}(|H\rangle + \mathrm{i}|V\rangle).
\end{aligned} \tag{15}$$

For the two time-bin qubits, the early state $|E\rangle$ denotes the input state $|T\rangle$ while the late state $|L\rangle$ denotes the input state $|T+\Delta T\rangle$. Then the states in the output port are

$$\begin{aligned}
|\mathrm{out}\rangle_{\mathrm{E}} &= \frac{1}{2}\left(|H\rangle_T - \mathrm{e}^{\mathrm{i}\varphi_2}|V\rangle_{T+\Delta T}\right),\\
|\mathrm{out}\rangle_{\mathrm{L}} &= \frac{1}{2}(|H\rangle_{T+\Delta T} - \mathrm{e}^{\mathrm{i}\varphi_2}|V\rangle_{T+2\Delta T}).
\end{aligned} \tag{16}$$

When choosing the states at time $T+\Delta T$, the output states are

$$|\mathrm{out}\rangle_{\mathrm{E}} = -\frac{1}{2}\mathrm{e}^{\mathrm{i}\varphi_2}|V\rangle = -\frac{1}{2}|V\rangle, \quad |\mathrm{out}\rangle_{\mathrm{L}} = \frac{1}{2}|H\rangle. \tag{17}$$

In the analysis above, there is no additional phase introduced by PS, i.e., $\varphi_2 = 0$. For other modulated phases, the results of the conversion are different. We list the conversion results in Table 4.

From the perspective of the application in an optical fiber system, the schematic of the time-bin phase to polarization converter is shown in Fig. 6. Set the slow (or fast) axes of the arms' PMFs align with the polarization direction of the PBS_1 and the PBS_2.

Table 4. The conversion results with different additional phases introduced by PS.

Phase of PS	0		$\pi/2$		π		$3\pi/2$	
	Basis	Bit flip?	Basis	Bit flip?	Basis	Bit flip?	Basis	Bit flip?
Time-bin phase	$X \to Y$	no	$X \to Z$	no	$X \to Y$	yes	$X \to Z$	yes
↓	$Y \to Z$	no	$Y \to Y$	no	$Y \to Z$	yes	$Y \to Y$	yes
Polarization	$Z \to X$	no	$Z \to X$	no	$Z \to X$	no	$Z \to X$	no

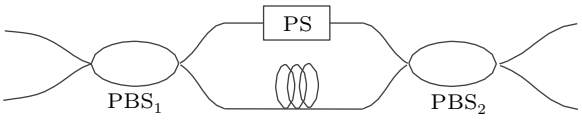


Fig. 6. Schematic of the time-bin phase to polarization converter based on commercial fiber-optic devices.

4. Conclusion

In this paper, we propose encoding conversion schemes between the polarization bases (rectilinear, diagonal and circular bases) and the time-bin phase bases (two phase bases and time-bin basis) and design the quantum encoding converters, which can help to achieve direct communication between the devices with different quantum encoding types. The conversion between polarization bases and time-bin phase bases can be easily selected by controlling a phase shifter. Our scheme can be applied to quantum communication systems encoded in any polarization states. Since no optical switches are used in our scheme, the converter can be operated with high speed. Moreover, the converters can be modularized, which may facilitate miniaturization in the future.

Acknowledgment

Project supported by the National Natural Science Foundation of China (Grant No. 62001440).

References

[1] Lo H K, Ma X and Chen K 2005 *Phys. Rev. Lett.* **94** 230504
[2] Lo H K, Curty M and Qi B 2012 *Phys. Rev. Lett.* **108** 130503
[3] Wang S, Chen W, Yin Z Q, He D Y, Hui C, Hao P L, Fan Yuan G J, Wang C, Zhang L J, Kuang J, Liu S F, Zhou Z, Wang Y G, Guo G C and Han Z F 2018 *Opt. Lett.* **43** 2030
[4] Chen J P, Zhang C, Liu Y, Jiang C, Zhang W, Hu X L, Guan J Y, Yu Z W, Xu H, Lin J, Li M J, Chen H, Li H, You L, Wang Z, Wang X B, Zhang Q and Pan J W 2020 *Phys. Rev. Lett.* **124** 070501
[5] Wang S, Yin Z Q, He D Y, Chen W, Wang R Q, Ye P, Zhou Y, Fan Yuan G J, Wang F X, Chen W, Zhu Y G, Morozov P V, Divochiy A V, Zhou Z, Guo G C and Han Z F 2022 *Nat. Photon.* **16** 154
[6] Ren J G, Xu P, Yong H L, *et al.* 2017 *Nature* **549** 70
[7] Ma X S, Herbst T, Scheidl T, Wang D, Kropatschek S, Naylor W, Wittmann B, Mech A, Kofler J, Anisimova E, Makarov V, Jennewein T, Ursin R and Zeilinger A 2012 *Nature* **489** 269
[8] Pirandola S, Eisert J, Weedbrook C, Furusawa A and Braunstein S L 2015 *Nat. Photon.* **9** 641
[9] Long G L and Liu X S 2002 *Phys. Rev. A* **65** 032302
[10] Pan D, Lin Z, Wu J, Zhang H, Sun Z, Ruan D, Yin L and Long G L 2020 *Photon. Res.* **8** 1522
[11] Liao S K, Cai W Q, Liu W Y, *et al.* 2017 *Nature* **549** 43
[12] Chen Y A, Zhang Q, Chen T Y, *et al.* 2021 *Nature* **589** 214
[13] Bennett C H and Brassard G 1984 *International Conference on Computers, Systems & Signal Processing*, December 9 12, 1984, Bangalore, India, p. 175
[14] Bennett C H and Brassard G 1989 *SIGACT News* **20** 78
[15] Elliott C 2002 *New J. Phys.* **4** 46
[16] Elliott C, Colvin A, Pearson D, Pikalo O, Schlafer J and Yeh H 2005 *Quantum Information and Computation III*, March 28 April 1, 2005, Orlando, Florida, p. 138
[17] Dianati M and Alleaume R 2007 *First International Conference on Quantum, Nano, and Micro Technologies (ICQNM'07)*, Jan 2 6, 2007, Guadeloupe, Guadeloupe, p. 13
[18] Dianati M, Alléaume R, Gagnaire M and Shen X Sherman 2008 *Security and Communication Networks* **1** 57
[19] Peev M, Pacher C, Alléaume R, Barreiro C, *et al.* 2009 *New J. Phys.* **11** 075001
[20] Sasaki M, Fujiwara M, Ishizuka H, *et al.* 2011 *Opt. Express* **19** 10387
[21] Agnesi C, Avesani M, Calderaro L, Stanco A, Foletto G, Zahidy M, Scriminich A, Vedovato F, Vallone G and Villoresi P 2020 *Optica* **7** 284
[22] Grünenfelder F, Boaron A, Rusca D, Martin A and Zbinden H 2018 *Appl. Phys. Lett.* **112** 051108
[23] Peng C Z, Zhang J, Yang D, Gao W B, Ma H X, Yin H, Zeng H P, Yang T, Wang X B and Pan J W 2007 *Phys. Rev. Lett.* **98** 010505
[24] Liu Y, Chen T Y, Wang J, Cai W Q, Wan X, Chen L K, Wang J H, Liu S B, Liang H, Yang L, Peng C Z, Chen K, Chen Z B and Pan J W 2010 *Opt. Express* **18** 8587
[25] Tang Z, Liao Z, Xu F, Qi B, Qian L and Lo H K 2014 *Phys. Rev. Lett.* **112** 190503
[26] Wang Z X, Xu H X, Li J, Yu H C, Huang J Q, Han H, Wang C L, Zhang P, Yin F F, Xu K, Liu B and Dai Y T 2025 *EPJ Quantum Technol.* **12** 47
[27] Muller A, Herzog T, Huttner B, Tittel W, Zbinden H and Gisin N 1997 *Appl. Phys. Lett.* **70** 793
[28] Gobby C, Yuan Z L and Shields A J 2004 *Appl. Phys. Lett.* **84** 3762
[29] Xu H X, Wang S H, Wang C L and Zhang P 2006 *Chin. Phys. Lett.* **42** 010303
[30] Tang G Z, Sun S H, Chen H, Li C Y and Liang L M 2016 *Chin. Phys. Lett.* **33** 120301
[31] Islam N T, Lim C C W, Cahall C, Kim J and Gauthier D J 2017 *Sci. Adv.* **3** 1701491
[32] Roberts G L, Lucamarini M, Dynes J F, Savory S J, Yuan Z L and Shields A J 2017 *Laser & Photonics Reviews* **11** 1700067
[33] Boaron A, Korzh B, Houlmann R, Boso G, Rusca D, Gray S, Li M J, Nolan D, Martin A and Zbinden H 2018 *Appl. Phys. Lett.* **112** 171108
[34] Lutkenhaus N 2024 (US Patent) 20040151321 [2004 8 5]
[35] Tamaki K, Lo H K, Fung C H F and Qi B 2012 *Phys. Rev. A* **85** 042307
[36] Bruß D 1998 *Phys. Rev. Lett.* **81** 3018
[37] Bennett C H 1992 *Phys. Rev. Lett.* **68** 3121
[38] Gisin N, Ribordy G, Tittel W and Zbinden H 2002 *Rev. Mod. Phys.* **74** 145